Formation of self-organized platinum nanoparticles and their microphotoluminescence enhancement in the visible light region

Chieh-Yu Kang, Cha-Hsin Chao, and Shu-Chia Shiu
Graduate Institute of Electro-Optical Engineering, National Taiwan University, Taipei, Taiwan 10617, Republic of China

Li-Jen Chou and Mu-Tung Chang
Department of Materials Science and Engineering, National Tsing Hua University, Hsinchu 30013, Republic of China

Gong-Ru Lin and Ching-Fuh Lin[a]
Graduate Institute of Electro-Optical Engineering, Graduate Institute of Electronics Engineering, and Department of Electrical Engineering, National Taiwan University, Taipei, Taiwan 10617, Republic of China

Formation of Pt nanoparticles or nanoisland films as a function of annealing temperature, initial thickness, underlying substrates, and annealing process is investigated. Using microphotoluminescence (PL) measurement, we find great enhancement of self-emission in visible spectrum from Pt nanoparticles. The integral intensity of the micro-PL of the 49.38 nm Pt nanoparticles is 38 times of that of the Pt thin film. In addition, the peak wavelength varies from 554 to 615 nm as the surface morphology of Pt changes due to different annealing parameters. Spectral analyses suggest that this enhancement of micro-PL from Pt is due to the local field enhancement mechanism analogous to that of PL from noble metals. © *2007 American Institute of Physics.*
[DOI: 10.1063/1.2785942]

I. INTRODUCTION

The unique optical properties of roughened metal surfaces or metal nanoparticles, especially of noble metals such as gold, silver, and copper, have been intensively studied over the past few decades. For instance, gold exhibits particular absorption peaks at visible wavelengths due to surface plasmon resonance (SPR) as its size is reduced to nanometer dimensions.[1] The Raman scattering of rhodamine 6G or other organic molecules adsorbed on aggregated Ag colloids can also be greatly enhanced.[2] This is the well-known phenomenon called surface enhanced Raman scattering (SERS).

Enhanced photoluminescence from noble metal nanoparticles has also been observed and has attracted much attention.[3] Theoretical work has previously demonstrated that the photoluminescence (PL) of noble metals is the direct recombination of the conduction-band electrons near the Fermi level with the holes in the d band.[4] However, the PL intensity of noble metals is very weak. The PL efficiency of smooth gold explored by Mooradian's original experiment was on the order of 10^{-10}. One possible reason for this low PL efficiency is that the nonradiative energy relaxation processes of photoexcited carriers in metals, such as Coulomb carrier-carrier scattering, are much faster than radiative electron-hole recombination, thus quenching the PL.[5] However, when noble metals are reduced to sizes in the range of nanometers, PL efficiency can be enhanced by about

$10^4 – 10^6$ times.[6] PL enhancement based on the phenomenological model by Boyd *et al.*[7] has been considered due to local field enhancement. Nonetheless, some scientists have developed different ideas in recent years. Dulkeith *et al.* explained a process in which the excited d-band holes recombined with the sp electrons emitting plasmons. These plasmons subsequently radiated, giving rise to PL.[8]

For transition metals, previous investigation has shown that their optical properties when they are several nanometers in size cannot be enhanced as significantly as those observed in Au, Ag, and Cu.[9] However, many applications and studies have been focused on them, particularly on Pt, which has been often used as electrode material. For example, roughened platinum electrodes can enhance the Raman scattering of pyridine[10] or other organic molecules; platinum island films can also enhance light absorption of some materials, such as infrared absorption of p-NTP.[11] A recent report demonstrated that Pt nanoparticles sputtered on ZnO can greatly enhance the bandgap emission of ZnO nanorods.[12] In this paper, we present an annealing method for fabricating Pt nanoisland films and nanoparticles of different sizes. The formation of nanoscale Pt particles as a function of temperature, film thickness, underlying substrates, and annealing process is reported. We have observed that the peak wavelength of surface enhanced micro-PL of Pt was shifted by the changes in the particles' shapes. X-ray photoelectron spectroscopy (XPS) and X-ray diffraction (XRD) were utilized to examine the composition of our samples. In order to observe the surface plasmon effect on our samples, the extinction spectra of Pt nanoisland films were measured.

---
[a] Author to whom correspondence should be addressed. Telephone: 886-2-3366 3540. FAX: 886-2-2364 2603. Electronic mail: cflin@cc.ee.ntu.edu.tw
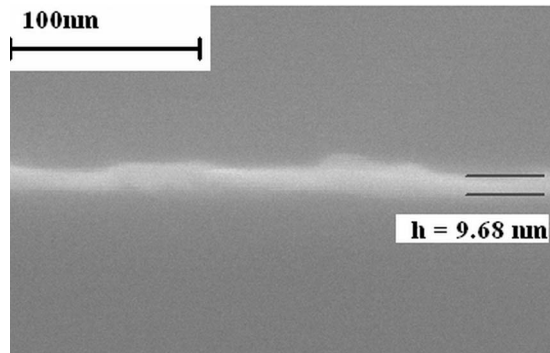
FIG. 1. SEM picture of unannealed Pt film.

II. EXPERIMENT

We produced our samples using platinum nanoparticles or nanoisland films on Si or quartz substrates. Si substrates were initially cleaned by acetone, methanol, and de-ionized water sequentially. Then, spin-on glass (SOG) 31F was spun on silicon substrates. The platinum film was deposited on SOG film by electron-gun evaporation at 1.8×10^{-6} torr. The deposition rate was estimated to be 0.01 nm/s. The scanning electron microscopy (SEM) photo of the unannealed Pt film is shown in Fig. 1. Its thickness is about 10 nm. The samples with the Pt thin film were then annealed at different temperatures. Different annealing apparatuses had also been tested. One used the rapid thermal annealing (RTA) with N_2 purging (RTA process) and the other used a heating stage in a chamber under a pressure of 10^{-3} torr (vacuum process). The purpose of the SOG film spun on the silicon substrates was to prevent the formation of PtSi alloy or other platinum silicides when the Pt thin film was annealed.[13] The samples on the quartz substrates were prepared by the same procedure as those on the Si substrates. After annealing for 5 min, Pt islands in the nanometer range were formed. The morphology and size distribution of the Pt nanoisland films were investigated using SEM. Micro-PL spectra of Pt nanoisland films were measured using excitation from a 514.5 nm Ar$^+$ laser focused through a microscope. The radiative emission was dispersed by a monochromator and detected by a cooled photomultiplier tube (PMT). The XRD studies were measured with a Cu Kα line and the XPS studies were carried out with an Mg Kα X-ray source (1253.6 eV). The extinction spectra of the platinum nanoisland films were also measured for the samples fabricated on the quartz substrates by a spectrophotometer with a resolution of 0.5 nm.

III. RESULTS AND DISCUSSION

SiO2 has a thermal expansion coefficient of 0.5×10^{-6}/K, which is much smaller than the thermal expansion coefficient of Pt films (8.8×10^{-6}/K). This would induce significant compressive stress in Pt (Ref. 14) when the Pt thin films were annealed. If the initial thickness of the metal is in the scale of nanometers, the compressive stress would cause the metal to form isolated islands.[15] In our works, the thickness of the Pt films and the annealing temperature have been varied to produce Pt nanoparticles and Pt nanoisland films with different sized particle. Figure 2 shows the SEM photos
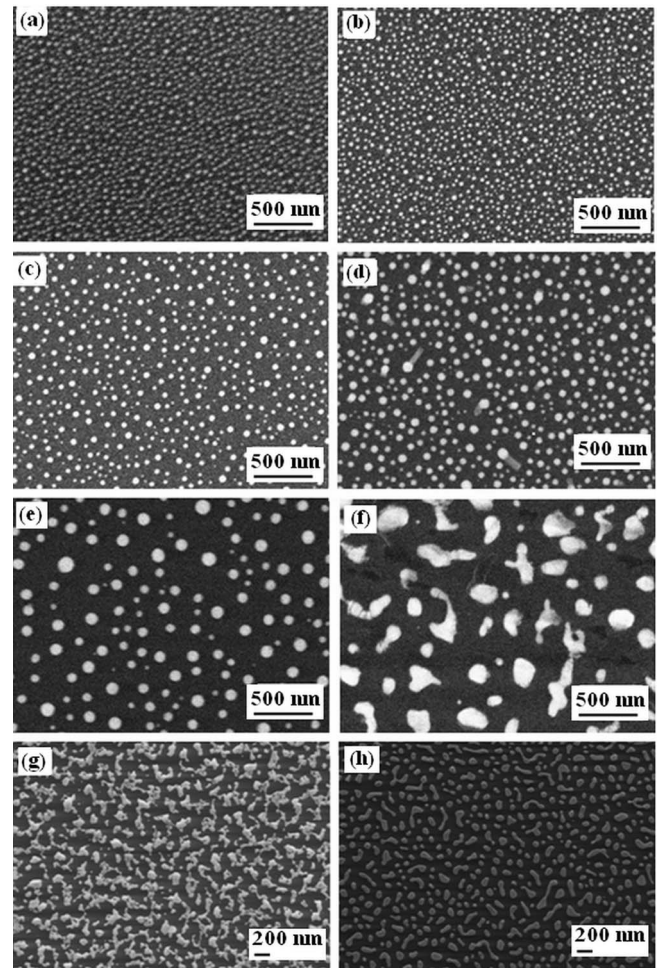

FIG. 2. SEM pictures of Pt nanoparticles and nanoisland films by different annealing methods. [(a)–(c)] 5 nm Pt thin film on the Si substrate annealed by the RTA process at 100, 1000, and 1200 K, respectively. [(d) and (e)] 10 nm Pt thin film on Si substrate annealed by the RTA process at 1000 and 1200 K, respectively. (f) 10 nm Pt thin film on Si substrate annealed by the vacuum process at 1000 K. (g) 10 nm Pt thin film on quartz substrate annealed by the vacuum process at 1000 K. (h) 10 nm Pt thin film on quartz substrate annealed by the RTA process at 1000 K.

of Pt nanoparticles and Pt nanoisland films with different sized particle. Figures 2(a)–2(c) are the SEM pictures of the 5 nm Pt thin film on the Si substrate annealed by the RTA process at 1000, 1100, and 1200 K, respectively. We found that the particle sizes increase with the annealing temperature. Figures 2(d) and 2(e) are the SEM pictures of the 10 nm Pt thin film on the Si substrate annealed by the RTA process at 1000 and 1200 K, respectively. They also reveal that the particle sizes formed at the higher temperature are larger than those formed at the lower temperature. Annealing at the high temperature allows mass transport of small clusters across the surface to form larger clusters in a process analogous to the Ostwald ripening mechanism.[16,17] Island formation mechanism analogous to Ostwald ripening could also be observed in our experiments. Figures 3(a) and 3(b) show feature variation in the surface morphology with the annealing temperature for those samples shown in Figs. 2(a)–2(e). Figure 3(a) demonstrates that average particle sizes increase with annealing temperature regardless whether the initial thickness of Pt is 5 or 10 nm. Figure 3(b) shows that island
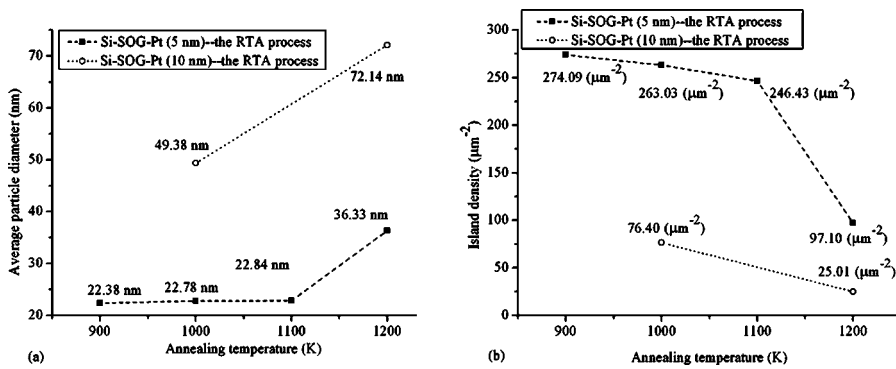
FIG. 3. (a) Average particle sizes at different annealing temperatures; (b) island density at different annealing temperatures.

density decreases with annealing temperature as well. It is clear that high annealing temperatures increase average particle size and reduce island density. Furthermore, Figs. 3(a) and 3(b) show that particle size suddenly increases and island density suddenly decreases at annealing temperatures above 1100 K for the Pt nanoparticles prepared with the 5 nm initial thickness. This may be attributed to surface melting of nanoparticles.[18] The fact that nanoparticle size remains at around 23 nm and then abruptly increases to 36 nm after 1100 K indicates that the melting point of the Pt nanoparticles with average diameter of 23 nm might be around 1100 K.

It is known that the initial thickness of the metal films can play an important role in determining their surface morphology at a given temperature.[19] From Fig. 3(a), the average diameter of the 5 nm initial thickness of Pt annealed at 1000 K is 22.78 nm. This is smaller than the 49.38 nm Pt nanoparticles prepared with 10 nm initial thickness. Figure 3(b) shows that when Pt thin film is annealed at 1000 K, the island densities are 263.03 μm^{-2} for the sample with 5 nm initial thickness and 76.40 μm^{-2} for the sample with 10 nm initial thickness. Similar results are shown in the Figs. 3(a) and 3(b) in which the samples were annealed at 1200 K as well. The thinner the initial film is, the larger the particle sizes and the higher the island density that are formed.

Previous studies have shown that the sizes of the metal islands are affected by different types of substrates[6,20] and different ambiences during the annealing process.[21] We investigated two processes, the vacuum process and the RTA process, and two different types of substrates, Si and quartz. Figures 2(f) and 2(g), respectively, show the SEM photos of the 10 nm Pt thin film on the Si substrate and the quartz substrate annealed by the vacuum process at 1000 K. Figures 2(d) and 2(h), respectively, show the SEM photos of the 10 nm Pt thin film on the Si substrate and the quartz substrate annealed by the RTA process at 1000 K. Our experi-

ments show that the island density of the Pt nanoisland films on quartz substrates is smaller than that on Si substrates both using the RTA and the vacuum process. In addition, the vacuum process results in a smaller island density than the RTA process, as shown in Table I.

The micro-PL of the Pt nanoparticles and the Pt nanoisland films was measured under the excitation of a 514.5 nm Ar^+ laser. Figure 4 shows the micro-PL spectra of several samples. Curves (a)–(c) are the micro-PL spectra of the Pt nanoparticles of different sizes prepared under different conditions. Curve (d) is the micro-PL of the sample of only SOG on Si without Pt. Curve (e) is the micro-PL spectrum of the 10 nm Pt thin film on Si substrate but without annealing. Curves (d) and (e) are shown together for comparison. The luminescence from the Pt nanoparticles is largely enhanced, when compared to the spectrum of the 10 nm Pt thin film without annealing. For instance, the integral intensity of the 49.38 nm Pt nanoparticles with the micro-PL spectrum shown by curve (a) in Fig. 4 is about 38 times of that of the sample with the 10 nm Pt thin film but without annealing. We also found that the peak wavelength of the micro-PL spectra of the Pt nanoparticles varies with their surface morphology. Similar phenomena have also been observed from gold nanoparticles and nanorods in previous studies.[22–24] It has been demonstrated that the PL enhancement of noble metal nanoparticles or rough surfaces is due to local field enhancement.[7,22] Local field enhancement includes two parts: One is the collective oscillation of electrons in surface protrusions which can be induced by the optical field. This is referred to as the local plasmon effect. The other is that field tends to concentrate at the tips of surface protrusions. This is known as the lightning rod effect, which is the reason for the redshift of emission peaks with the increasing aspect ratio of nanorods.[7,22,23] From our results, as shown in Fig. 4, we find that the peak wavelengths of curves (a) and (b) are close to 554 nm, but the peak wavelength of curve (c) is significantly

TABLE I. Island formation conditions using the RTA and the vacuum processes.

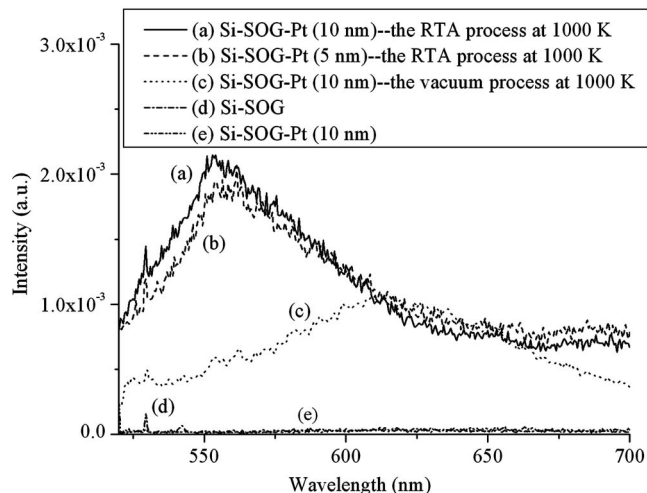| Substrates	Initial thickness (nm)	Annealing temperature (K)	Process	Island density (μm^{-2})	SEM image
Si	10	1000	RTA	76.40	Fig. 2(d)
Si	10	1000	Vacuum	9.51	Fig. 2(f)
Quartz	10	1000	Vacuum	9.12	Fig. 2(g)
Quartz	10	1000	RTA	26.84	Fig. 2(h)

FIG. 4. The micro-PL spectra of samples on Si substrates with (a) the 10 nm Pt thin film annealed by the RTA process at 1000 K, (b) the 5 nm Pt thin film annealed by the RTA process at 1000 K, (c) the 10 nm Pt thin film annealed by the vacuum process at 1000 K, (d) the SOG film, and (e) the 10 nm Pt thin film without annealing.

redshifted to 610 nm. The particles whose micro-PL spectra are shown in Figs. 4(a) and 4(b) are almost round in shape. The aspect ratio of the Pt nanoparticles is obviously smaller than that of the Pt nanoisland films. As a result, the redshift of the peak wavelength of the micro-PL from the Pt nanoisland films is to be expected. We suggest that the variation of the peak wavelength of the micro-PL from Pt is due to the lightning rod effect.

The enhanced micro-PL of Pt can be found in the Pt nanoisland films on the quartz substrates as well, as shown in Fig. 5 In Figs. 5(a) and 5(b) are shown the micro-PL spectra of the Pt nanoisland film formed by the RTA process and the vacuum process, respectively. Curve (c) is the micro-PL spectra of the 10 nm Pt thin film on the quartz substrate without annealing. From Fig. 5, the integral intensity of the micro-PL spectrum shown by curve (a) for the Pt nanoisland film (island density of 26.84 μm^{-2}) is about eight times of
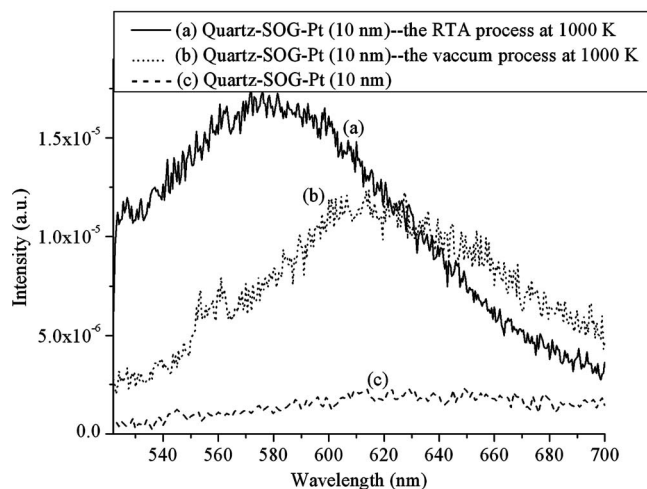

FIG. 5. The micro-PL spectra of the samples on quartz substrates with (a) the 10 nm Pt thin film annealed by the RTA process at 1000 K, (b) the 10 nm Pt thin film annealed by the vacuum process at 1000 K, and (c) the 10 nm Pt thin film without annealing.
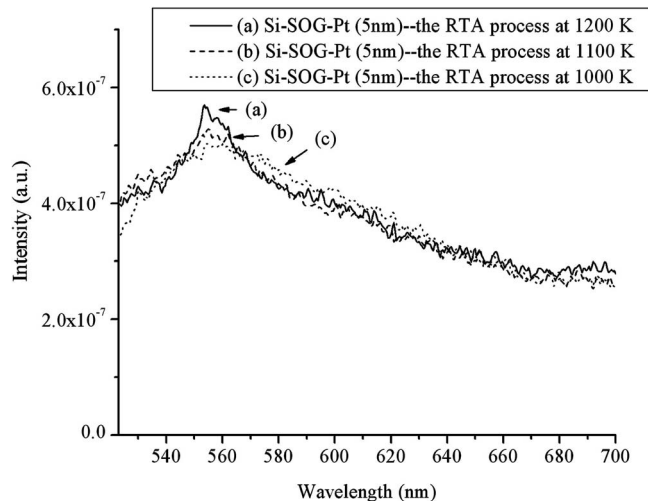

FIG. 6. The micro-PL spectra for the samples with 5 nm initial thickness annealed at different temperatures by the RTA process. (a) The annealing temperature is 1200 K. (b) The annealing temperature is 1100 K. (c) The annealing temperature is 1000 K.

that of the sample with the 10 nm Pt thin film without annealing. In addition, the variation of the peak wavelength of the micro-PL due to different surface morphologies of Pt can be found. The peak wavelength of the micro-PL of the Pt nanoisland film annealed by the RTA process is about 576 nm, and for the sample annealed by the vacuum process, it is close to 615 nm. Figure 6 shows the micro-PL spectra of the samples with 5 nm initial thickness of Pt annealed at different temperatures. Curves (a)–(c) in Fig. 6 show the samples annealed by the RTA process at 1200, 1100, and 1000 K, respectively. The peak wavelengths of the micro-PL spectra are all close to 554 nm. This is due to the fact that the particles of the samples with the 5 nm initial thickness of Pt annealed at temperatures higher than 1000 K are almost round. This micro-PL is significantly enhanced by the Pt nanomorphology.

Similar results showing intense fluorescence from transition-metal nanoparticles such as Fe have been reported.[25] The authors suggest that the partial oxidation of metal nanoparticles possibly occur on the metal's surface. These metal oxide clusters are photoactivated and might give rise to the observed fluorescence. In order to confirm the composition of the Pt nanoparticles and the nanoisland films, the XPS and XRD measurements are utilized. The XPS studies were carried out with a Mg $K\alpha$ x-ray source (1253.6 eV). One of our samples' XPS spectra is shown in Fig. 7. This illustrates the sample with 10 nm Pt thin film annealed by the RTA process at 1000 K. The XPS peaks in Fig. 7 are referenced to the C 1s binding energy of the adventitious carbon at 284.5 eV. Figure 7(a) is the XPS spectrum in the range between 0 and 600 eV. All the peaks are labeled and reveal that three elements, Pt, Si, and O, exist at the surface of the samples. To get a clear view, the XPS spectrums of Si 2p and Pt 4f are plotted in Figs. 7(b) and 7(c), respectively. From Fig. 7(b), the peak of Si 2p is at 103.43 eV, which is originated from the SOG film under the Pt nanoparticles. From Fig. 7(c), the peak of Pt $4f_{7/2}$ is at 71.11 eV. The fact that the binding energy of the Pt $4f_{7/2}$ peak for the bulk Pt measured
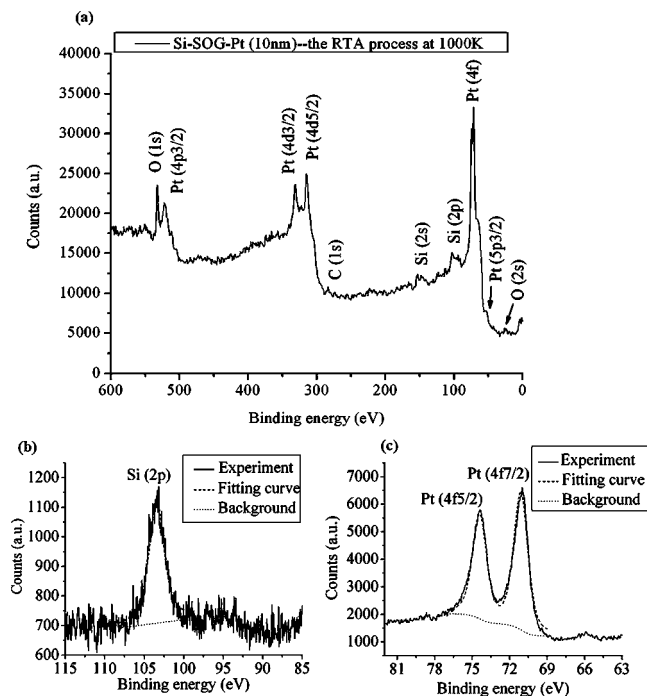
FIG. 7. The XPS spectra for the sample with the 10 nm Pt thin film annealed by the RTA process at 1000 K. (a) The XPS spectrum in the range of 0–600 eV. (b) The XPS spectrum for Si 2p. (c) The XPS spectrum for Pt 4f.

by the same instrument is 71.3 eV suggests that oxidation and silicide formation on Pt nanoparticles during annealing do not occur. Figure 8 shows the result of the XRD of the Pt nanoisland films on the quartz substrates annealed by different processes. Only the XRD signal corresponding to Pt (111) is found. The broad XRD signal of a-PtO$_x$ ($2\theta=32°$) (Ref. 26) and the XRD signals of PtSi or Pt$_2$Si (Ref. 27) are not observed. The results show that the SOG films under the Pt thin film could prevent the formation of platinum silicide and platinum oxide during annealing. This result is in line with previous research.[13] The investigation using the XPS and XRD measurements suggests that the composition of the
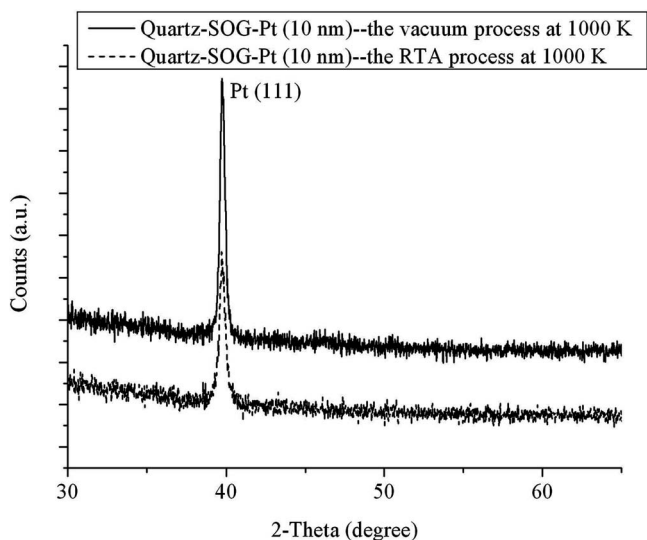

FIG. 8. The XRD spectra of the Pt nanoisland films annealed by different processes. Only the peak corresponding to Pt (111) is found.

nanoisland films and the nanoparticles mainly consist of Pt. As a result, we believe that their optical properties as measured by micro-PL should be related to their surface morphology.

Since the results of the XPS and the XRD show that the nanoparticles and the nanoisland films are composed of Pt, we suggest that the origin of micro-PL from Pt might be attributed to d-band and sp-band transitions. The mechanism is analogous to that of noble metals. The characteristics of the d band of Pt are not like those of noble metals, which lie deeply under the Fermi level. The d band of Pt extends into the Fermi level and over about 0.3 eV.[28,29] Since the Coulomb carrier-carrier scattering time considerably depends on the density of states (DOS) around the Fermi level, and the DOS around the Fermi level is enhanced by the d states in Pt, the lifetime of the photoexcited carriers is smaller in Pt than in noble metals.[30] This significantly reduces the radiative electron-hole recombination in the smooth Pt film. For this reason, the signal of emission is very low and could not be easily detected from the Pt thin films in our experiment. However, as nanoparticles and the nanoisland films are formed after annealing, the efficiency of the light coming from Pt can be greatly improved because of the local field enhancement mechanism.

The extinction spectra of Pt nanoisland films on quartz substrates were measured to observe the localized surface plasmon effect in our samples with the quartz substrates. Localized surface plasmon resonance (LSPR) is the excitation of collective resonance of conduction electrons induced by electromagnetic radiation.[31–33] The frequency of the LSPR can be tuned by changing the size, shape, and dielectric constant of the surrounding medium.[31–33] For platinum, previous studies had shown that the frequency of the LSPR is located in the ultraviolet light region.[13,22] Nonetheless, recently, Langhammer et al.[33] reported that the extinction peak of a Pt nanodisk would shift from 200 to 1800 nm as the diameters varied from 38 to 530 nm. Figures 9(a) and 9(b) are the extinction spectra of the samples with the 10 nm Pt thin film annealed by the RTA and the vacuum processes at 1000 K. The SOG film on the quartz substrate is used as a reference, indicating that the extinction features result from the platinum nanoisland films. Figure 9(a) shows that there are extinction peaks at 230 and 330 nm for the sample annealed by the RTA process at 1000 K. Figure 9(b) shows that the extinction peaks are at 330 and 512 nm for the sample annealed by the vacuum process at 1000 K. These peaks are referred to as the frequency of the LSPR of the Pt nanoisland films. The characteristics of the two peaks in the extinction spectra might be attributed to the resonant frequency of the transverse and the longitudinal plasmon oscillation.[22–24] Since the frequency of the LSPR of metal nanostructures is redshifted with increasing particle size and aspect ratio,[22–24,33] the extinction spectra in Figs. 9(a) and 9(b) reveal that the particle size and the aspect ratio of the Pt nanoisland films annealed by the vacuum process are larger than those of the Pt nanoisland films annealed by the RTA process. This result corresponds to their surface morphology, as shown in the SEM pictures [Figs. 2(g) and 2(h)] and their micro-PL behaviors [curves (a) and (b) in Fig. 5]. In addi-
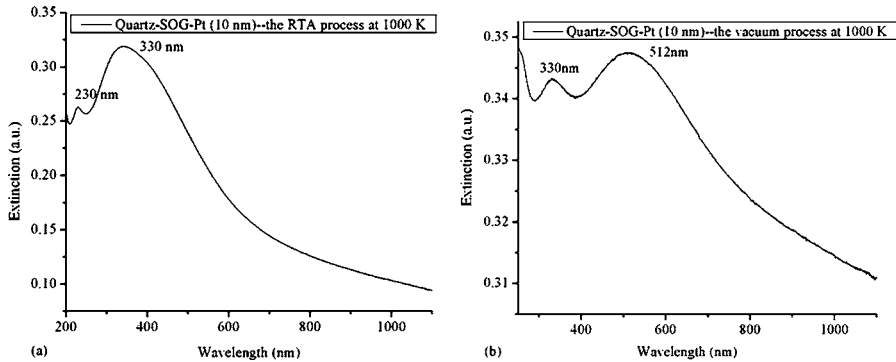
FIG. 9. The extinction spectra of the samples on quartz substrates with (a) the 10 nm Pt thin film annealed by the RTA process at 1000 K and (b) the 10 nm Pt thin film annealed by the vacuum process at 1000 K.

tion, we could not find a peak near 1.2–1.4 eV from the extinction spectra, which is assigned to the absorption peak of PtO_x.[34,35] We can confirm that the extinction features result from the surface morphology of Pt.

Some research has suggested that the PL of noble metals might be related to the resonance of surface plasmon. Dulkeith *et al.*[8] reported that the emission spectra of gold nanoparticles could coincide with their extinction spectra according to the Mie theory, so they stated that PL enhancement should be due to the emission of particle plasmons. Mohamed *et al.*[23] suggested that the relaxation of surface plasmon coherent electronic motions followed by the recombination of the *d*-band holes and the *sp*-band electrons lead to the enhanced PL of gold since the wavelength of the LSPR was close to that of their excitation laser. However, Varnavski *et al.*[24] found that the luminescence efficiency is the same for gold nanospheres (with a surface plasmon resonance of 520 nm) when using an excitation laser at 4.65 and 3.02 eV. Their experimental results are inconsistent with the suggestion that the observed emission is due to surface plasmon emission or surface plasmon excitation by incoming light. They reported that the emission originated from the *sp*-electron/*d*-hole recombination with the enhancement of the incoming and outgoing fields via the local field enhancement mechanism. From our extinction spectra, as shown in Fig. 9, one of the LSPR for the Pt nanoisland films annealed by the vacuum process is 512 nm. This is close to the wavelength of our excitation laser (514.5 nm). This result shows the possibility that the micro-PL enhancement could be related to the excitation of the LSPR. However, for the sample annealed by the RTA process, the LSPR differs greatly from the wavelength of our excitation laser and the peak position of the micro-PL. If the observed micro-PL comes from LSPR excitation, the signal of micro-PL from the sample annealed by the vacuum process should be larger than that from the sample annealed by the RTA process. Nevertheless, our experimental results contradict this. The integral intensity of the micro-PL for the sample annealed by the vacuum process is lower than that of the sample annealed by the RTA process. These results reveal that the observed micro-PL of Pt would not be significantly influenced by the behaviors of the LSPR. The excitation of the LSPR might contribute to the enhancement of micro-PL for the sample annealed by the vacuum process, but whether the LSPR is crucial to the observed micro-PL could not be easily confirmed by our investigation. As a result, we suggest that the observed micro-PL of Pt is attributed to the local field enhancement of the incoming and outgoing fields.

IV. CONCLUSIONS

In summary, we used the annealing process to produce Pt nanoparticles or Pt nanoisland films of different sizes as a function of temperature, film thickness, pressure, and underlying substrates. The high annealing temperature caused particle size to increase and island density to decrease. Increasing the initial thickness of Pt from 5 to 10 nm, we found that the particle sizes doubled and island density was reduced. The quartz substrates resulted in a smaller island density than the Si substrates and the vacuum process produced a smaller island density than the RTA process. Furthermore, our experiment suggests that the melting point of the 23 nm Pt nanoparticles is about 1100 K. In addition, we found that the surface enhanced micro-PL of Pt is analogous to the PL of noble metal nanoparticles. The integral intensity of the micro-PL of the 49.38 nm Pt nanoparticles is 38 times of that of the Pt thin film. The peak wavelength of the micro-PL of the Pt nanoparticles varied from 554 to 615 nm as a result of the change in the Pt surface morphology. Extinction spectra show that the frequency of the LSPR for the Pt nanoisland film annealed by the RTA process is at 230 and 330 nm. Those peaks redshift to 330 and 512 nm for the Pt nanoisland film annealed by the vacuum process. The redshift of the extinction peaks reveals that the particle size and the aspect ratio of the Pt nanoisland film annealed by the vacuum process are larger than those of the Pt nanoisalnd film annealed by the RTA process. This result corresponds to their surface morphology, as shown by the SEM pictures and their micro-PL behaviors. From our studies of the XPS and the XRD, we suggest that the observed optical properties of the Pt nanoparticles and the nanoisland films are related to their surface morphology. Our results for the optical properties of Pt nanoparticles measured by micro-PL and extinction could lead to a wide range of potential applications, including solar cells and surface enhanced Raman scattering.

[1] M. M. Alvarez, J. T. Khoury, T. G. Schaaff, M. N. Shafigullin, I. Vezmar, and R. L. Whetten, J. Phys. Chem. B **101**, 3706 (1997).
[2] A. M. Michaels, M. Nirmal, and L. E. Brus, J. Am. Chem. Soc. **121**, 9932 (1999).
[3] M. Moscovits, Rev. Mod. Phys. **57**, 783 (1985).
[4] A. Mooradian, Phys. Rev. Lett. **22**, 185 (1969).
[5] T. Qiu, X. L. Wu, and Y. C. Cheng, Appl. Phys. Lett. **88**, 143111 (2006).
[6] L. Khriachtchev, L. Heikkila, and T. Kuusela, Appl. Phys. Lett. **78**, 1994 (2001).
[7] G. T. Boyd, Z. H. Yu, and Y. R. Shen, Phys. Rev. B **33**, 7923 (1986).
[8] E. Dulkeith, T. Niedereichholz, T. A. Klar, J. Feldmann, G. von Plessen, D. I. Gittins, K. S. Mayya, and F. Caruso, Phys. Rev. B **70**, 205424 (2004).
[9] Z. Q. Tian, B. Ren, and D. Y. Wu, J. Phys. Chem. B **106**, 9463 (2002).
[10] W. B. Cai, B. Ren, X. Q. Li, C. X. She, F. M. Liu, X. W. Cai, and Z. Q. Tian, Surf. Sci. **406**, 9 (1998).
[11] A. E. Bjerke and P. R. Griffiths, Appl. Spectrosc. **56**, 1275 (2002).
[12] J. M. Lin, H. Y. Lin, C. L. Cheng, and Y. F. Chen, Nanotechnology **17**, 4391 (2006).
[13] E. Anno and M. Tanimoto, J. Appl. Phys. **88**, 3426 (2000).
[14] C. Bower, O. Zhou, W. Zhu, D. J. Werder, and S. Jin, Appl. Phys. Lett. **77**, 2767 (2000).
[15] J. A. Floro, S. J. Hearne, J. A. Hunter, P. Kotula, E. Chason, S. C. Seel, and C. V. Thompson, J. Appl. Phys. **89**, 4886 (2001).
[16] J. D. Carey, L. L. Ong, and S. R. P. Silva, Nanotechnology **14**, 1223 (2003).
[17] S. Wei, B. Li, T. Fujimoto, and I. Kojima, Phys. Rev. B **58**, 3605 (1998).
[18] Z. L. Wang, J. M. Petroski, T. C. Green, and M. A. El-Sayed, J. Phys. Chem. B **102**, 6145 (1998).
[19] S. Aggarwal, S. B. Ogale, C. S. Ganpule, S. R. Shinde, V. A. Novikov, A. P. Monga, M. R. Burr, R. Ramesh, V. Ballarotto, and E. D. Williams, Appl. Phys. Lett. **78**, 1442 (2001).
[20] T. L. Alford, L. Chen, and K. S. Gadre, Thin Solid Films **429**, 248 (2003).
[21] A. S. Eppler, G. Rupprechter, E. A. Anderson, and G. A. Somorjai, J. Phys. Chem. B **104**, 7286 (2000).
[22] S. Link and M. A. El-Sayed, Annu. Rev. Phys. Chem. **54**, 331 (2003).
[23] M. B. Mohamed, V. Volkov, S. Link, and M. A. El-Sayed, Chem. Phys. Lett. **317**, 517 (2000).
[24] O. P. Varnavski, T. Goodson III, M. B. Mohamed, and M. A. El-Sayed, Phys. Rev. B **72**, 235405 (2005).
[25] A. Alqudami and S. Annapoorni, Plasmonics **2**, 5 (2007).
[26] K. L. Saenger, C. Cabral, Jr., C. Lavoie, and S. M. Rossnagel, J. Appl. Phys. **86**, 6084 (1999).
[27] A. A. Naem, J. Appl. Phys. **64**, 4161 (1988).
[28] N. V. Smith, Phys. Rev. B **9**, 1365 (1974).
[29] R. E. Dietz, E. G. McRae, and J. H. Weaver, Phys. Rev. B **21**, 2229 (1980).
[30] N. Pontius, M. Neeb, W. Eberhardt, G. Luttgens, and P. S. Bechthold, Phys. Rev. B **67**, 035425 (2003).
[31] D. Dalacu and L. Martinu, J. Opt. Soc. Am. B **18**, 85 (2001).
[32] A. Hilgera, N. Cuppers, M. Tenfelde, and U. Kreibig, Eur. Phys. J. D **10**, 115 (2000).
[33] C. Langhammer, Z. Yuan, I. Zoric, and B. Kasemo, Nano Lett. **6**, 833 (2006).
[34] H. Neff, S. Henkel, E. Hartmannsgruber, E. Steinbeiss, W. Michalke, K. Steenbeck, and H. G. Schmidt, J. Appl. Phys. **79**, 7672 (1996).
[35] C. R. Aita and Ngoc C. Tran, J. Appl. Phys. **56**, 958 (1984).